GLUCOSE DEPLETION DECREASES CELL VIABILITY WITHOUT TRIGGERING DEGENERATIVE CHANGES IN A PHYSIOLOGICAL NUCLEUS PULPOSUS EXPLANT MODEL

Mathilde Padrona, Manon Maroquenne, Hanane El-Hafci, Lucille Rossiaud, Hervé Petite, Esther Potier

GLUCOSE DEPLETION DECREASES CELL VIABILITY WITHOUT TRIGGERING DEGENERATIVE CHANGES IN A PHYSIOLOGICAL NUCLEUS PULPOSUS EXPLANT MODEL

Authors : Mathilde PADRONA[1], Manon MAROQUENNE[1], Hanane EL-HAFCI[1], Lucille ROSSIAUD[1], Hervé PETITE[1], and Esther POTIER[1*]

Affiliations:

1: Université Paris Cité, CNRS, INSERM, ENVA, B3OA, F-75010 Paris, France

Key words: Glucose deprivation/depletion; Nucleus pulposus; Nucleus pulposus homeostasis; Physiological culture model; Intervertebral disc degeneration

Abstract: Although the etiology of intervertebral disc degeneration is still unresolved, the nutrient paucity resulting from its avascular nature is suspected of triggering degenerative processes in its core: the nucleus pulposus (NP). While severe hypoxia has no significant effects on NP cells, the impact of glucose depletion, such as found in degenerated discs (0.2 - 1 mM), is still uncertain. Using a pertinent ex vivo model representative of the unique disc microenvironment, the present study aimed, therefore, at determining the effects of "degenerated" (0.3 mM) glucose levels on bovine NP explant homeostasis. The effects of glucose depletion were evaluated on NP cell viability, apoptosis, phenotype, metabolism, senescence, extracellular matrix anabolism and catabolism, and inflammatory mediator production using fluorescent staining, RT-qPCR, (immuno)histology, ELISA, biochemical, and enzymatic assays. Compared to the "healthy" (2 mM) glucose condition, exposure to the degenerated glucose condition led to a rapid and extensive decrease in NP cell viability associated with increased apoptosis. Although the aggrecan and collagen-II gene expression was also downregulated, NP cell phenotype, and senescence, matrix catabolism, and inflammatory mediator production were not, or only slightly, affected by glucose depletion. The present study provided evidence for glucose depletion as an essential player in NP cell viability but also suggested that other micro-environment factor(s) may be involved in triggering the typical shift of NP cell phenotype observed during disc degeneration. The present study contributes new information for better understanding disc degeneration at the cellular-molecular levels and thus helps to develop relevant therapeutical strategies to counteract it.

Introduction:

In 2017, low back pain was considered the leading cause of long-term disability in 195 countries, requiring medical treatments and extended sick-leaves that resulted in substantial socio-economic burdens.[1,2] This painful and debilitating symptom is significantly associated with degeneration of the intervertebral discs (IVDs).[3,4] IVDs comprise a gelatinous core, the nucleus pulposus (NP), surrounded by a fibrous outer layer, the annulus fibrosus, and endplates at the vertebral interface. IVD degeneration initiates in the NP and is characterized by extracellular matrix (ECM) degradation, constituent cell loss, change in the surviving cell phenotype, and release of inflammatory mediators.[5]

Although the etiology of IVD degeneration is still unresolved, IVD nutrient paucity is suspected of playing a critical role. Because of its avascular nature, IVD indeed solely relies on diffusion of oxygen and nutrients from blood capillaries ending in the endplates and the outer annulus fibrosus; the result is physiologically low concentrations of oxygen (between 0.3 and 7.9%)[6] and glucose (between 0.6 and 3.1mM)[7–9] in the healthy NP. Likewise, removal of metabolic wastes is limited and contributes to an acidic NP environment (between 7.1 and 7.5).[10] Several endplate modifications associated with IVD degeneration, such as sclerosis of the bony layer or calcification and dehydration of the cartilaginous layer, are suspected to compromise this precarious diffusive route and aggravate nutrient meagreness in IVD.[11] There are, however, very few literature reports of experimental in situ characterization of human, degenerated NP micro-environment. One study reported oxygen values as low as 0.7%[12] and another one an average glucose concentration of 0.6 ± 0.1mM[13]. Additionally, theoretical models incorporating reduced endplate permeability estimated minimal oxygen levels at 0.2 - 0.3% and minimal glucose concentrations at 0.16 - 0.35 mM.[7,14,15]

This nutrient paucity prompted the evaluation of the effects of oxygen and glucose depletion on NP cells in order to elucidate the underlying disc degeneration mechanisms. Severe (i.e., 0 or 1% pO_2) hypoxia has no-to-little effects on bovine NP cell viability.[16–19] In contrast, total glucose depletion (i.e., 0 mM) had a drastic effect evidenced by significant decrease in rat, bovine, and human NP cell viability and anabolic gene expression levels.[16, 20–23] While these studies are interesting, total glucose depletion, as they used, is not representative of the glucose levels that are found in degenerated IVD. Such glucose levels (i.e., 0.2 - 1mM of glucose), in fact, led to inconsistent results regarding bovine and porcine NP cell viability and ECM turnover, with negative and no effects reported.[13,16,19,22,24,25] These discrepancies may be explained by different pO_2 and pH levels (from 0 to 21% and 6.2 to 7.4, respectively) used in these studies when oxygen and pH strongly affect IVD cell metabolism[26,27] and response to glucose depletion[28]. Another explanation may also be cell dedifferentiation in some of the aforementioned studies when NP cells are expanded prior to experimentation.[29]

Moreover, all the cited studies used cells isolated from their native ECM. ECM, however, provides not only mechanical support for cells and for tissue integrity but also plays a crucial role in cell survival, proliferation, and differentiation.[30] It can dictate NP cell's response to glucose depletion by sequestering and regulating several types of growth factors acting on local cell populations[31], by triggering intracellular signaling pertinent to cell phenotype through integrin binding[32], and/or by acting as both agonists and antagonists of soluble growth factors, such as transforming growth factor-β family ligands[33].

Thus, to better understand the effects of glucose depletion on NP homeostasis, the present study used a physiologically relevant bovine NP explant culture model where NP cells are maintained in their native ECM and cultured in controlled, physiological conditions (4.4% pO_2, 430 mOsm/kg H_2O, and pH 7.1) representative of the unique IVD microenvironment. The effects of physiological glucose levels representative of healthy (2 mM) or degenerated (0.3 mM) IVD on bovine NP cell viability, phenotype, senescence, apoptosis, ECM anabolism, and catabolism, as well as production of select inflammatory mediators, were evaluated.

Materials and Methods:

Experimental plan

Bovine NP explants were cultured under two glucose conditions considered physiological in human healthy and degenerated NP, specifically, 2 mM[7–9] and 0.3 mM[7,14,15], respectively. NP cell viability and ECM content were first assessed at 1, 5, 8, 12, and 21 days of NP explant culture (n = 8 donors). At each time point of analysis, each NP was cut in two: one half was analyzed for cell viability (using fluorescent staining and confocal imaging); the other half was evaluated for water, glycosaminoglycans (GAG), and collagen contents (using biochemical assays). Based on the results obtained in this first part of the study, the effects of glucose depletion on NP homeostasis were further assessed after 1, 5, and 12 days of NP explant culture (n = 6 donors). At each time point of analysis, NP were cut in two: one half was used to determine expression levels of genes involved in NP cell senescence and phenotype, ECM anabolism and catabolism, and glucose transport (using RT-qPCR); the other half was used to characterize cell apoptosis and proteoglycan and collagen composition (using (immuno)histology). For each assay, fresh NP explants served as D0 controls. At every culture medium change, aliquots of the supernatant media were collected and analyzed for glucose, lactate, select inflammatory mediators (specifically, interleukin-1β (IL-1β), interleukin-6 (IL-6), and tumor necrosis factor-α (TNF-α)) contents, and for determination of total matrix metalloproteinases (MMP) released (using biochemical assays).

Bovine NP explant culture

Bovine caudal IVDs were obtained from a local slaughterhouse within 24 hours of animal death. All biological specimens from the slaughterhouse were obtained in accordance with local regulations. Briefly, bovine tails were dissected and cut into motion segments, keeping the five highest levels. Under sterile conditions, the motion segments were opened transversally, directly underneath the cartilaginous endplate. NP specimens were harvested using an 8-mm-diameter biopsy punch and directly placed in culture medium. Using an explant culture system previously described[34,35], NP explants were placed in a semipermeable membrane (Spectra/Por® 15 kDa molecular weight cut-off, Spectrum Laboratories, Rancho Dominguez, CA, USA) and closed using custom-made plastic rings and were cultured in either physiological healthy (2mM) or degenerated (0.3mM) glucose conditions.

The cell culture media were basic Dulbecco's Modified Eagle Medium without glucose (Gibco™, Thermo Fischer Scientific, Waltham, MA USA) supplemented with 1% penicillin/streptomycin (Pan Biotech, Aidenbach, Germany), 3-(N-morpholino)propanesulfonic acid 20 mM (Sigma-Aldrich™, Merck, Fontenay sous Bois, France), and 6.65% of FBS (Dominique Dutscher, Bernolsheim, France), corresponding to 0.3 mM of glucose as measured with an automated analyzer (Respons 910, Dyasis Diagnostic Systems GmbH, Holzheim, Germany). The physiological healthy glucose concentration (2 mM) was achieved by supplementing the FBS-containing culture medium with 1.7 mM D-glucose (Sigma-Aldrich™). Cell culture media osmolarity was set at healthy value (420-430 mOsm/kg H2O)[10] adding 11% polyethylene glycol (Sigma-Aldrich™) for both culture conditions and osmolarity was confirmed using an automated freezing point osmometer (A2O®, Radiometer, Copenhagen, Denmark). pH (7.1), as well as environmental pO2 (4.4%), were also set at healthy physiological values in order to only assess the effects of glucose depletion.[6,10] All media were filter-sterilized and stabilized by maintenance at 37°C, 4.4% pO2, and 10% pCO2 for 48h before use in experiments. During the 12 and 21 days of cell culture, culture media were changed two times a week for both culture conditions, using a hypoxic glove box to ensure stable pO2 throughout the experiment.

Cell staining and confocal imaging

Cell viability and cell death were determined using calcein-AM and propidium iodide staining, respectively. Samples were rinsed twice in phosphate-buffered saline (PBS) and incubated first in 1 µg/mL calcein-AM (Sigma-Aldrich™) in PBS at 4°C for 1 hour and then at 37°C for 30 min. Propidium iodide (Sigma-Aldrich™) was added at 1 µg/mL for the last 5 minutes of incubation at 37°C. The stained samples were rinsed twice in PBS and imaged using a laser-free confocal microscope (TE2000-U, Nikon, Badhoevedorp, The Netherlands linked with confocal imager Clarity, Aurox, Abingdon, United Kingdom and digital

camera ORCA Flash 4.0, Hamamatsu Photonics, Massy, France) at λ ex = 466/40 nm and λ em = 525/45 nm for calcein-AM and λ ex = 554/23 nm and λ em 609/54 nm for propidium iodide. For each sample, stacks between 700 and 1,300 µm of depth were analyzed at two random spots and manually counted using FIJI software (FIJI 2.1.0/1.53q; Java 1.8.0_172 [64-bit])[36], with a minimum of 200 total cells randomly counted per specimen. Cell viability was determined as the living cell number divided by the total (dead and living) cell number.

Biochemical assays

NP samples were weighed (wet weight) and stored at -80°C until further analysis. At the time of analysis, these samples were lyophilized overnight (Alpha™ lyophilizer, Christ Martin, Osterode am Harz, Germany) and then weighed again (dry weight). The water content was calculated from the difference in the respective wet and dry weights divided by the wet weight. Each lyophilized sample was then digested using a digestion buffer (100 mM phosphate buffer, 5 mM L-cysteine, 5 mM ethylene diamine tetraacetic acid, and 125-140 µg/mL papain (all Sigma-Aldrich™) at 60°C, overnight. The digested samples were then used to determine total sulphated GAG content using the 1,9-dimethyl methylene blue (Sigma Aldrich™) dye-binding assay.[37] The hydroxyproline (HYP) content was determined using the Chloramine-T (Sigma Aldrich™) assay.[38] The amounts of GAG and HYP were expressed per mg of tissue dry weight.

Histology and immunohistochemistry

NP samples were fixed in 4% paraformaldehyde (Sigma Aldrich™) at room temperature for 24 hours, dehydrated, and embedded in paraffin using a tissue processor (STP 120 Spin, Epredia, Portsmouth, NH, USA). 5 µm-thick sagittal sections were then cut in the central zone of the explants and stained with safranin-O solution (0.1% w/v in milliRo water, Sigma Aldrich™), Fast-Green solution (0.01% w/v in milliQ water, Sigma Aldrich™), and Weigert's Iron Hematoxylin (mixed in equal parts of 10 mg/mL hematoxylin (Sigma Aldrich™) in 95° ethanol (Fluka) solution, iron III chloride (Sigma Aldrich™) 1.16% w/v, and hydrochloric acid (Sigma Aldrich™) 0.37% w/v in milliRo water) for proteoglycans, collagens, and cell nuclei, respectively. Images of stained samples were taken with a digital microscope (VHX-2000, Keyence, Bois-Colombes, France). For D12 samples, apoptosis was evaluated using Click-iT™ Plus terminal deoxynucleotidyl transferase-dUTP nick end labeling (TUNEL) Assay Kits for In Situ Apoptosis Detection with Alexa Fluor dyes according to the manufacturer's (Invitrogen™, Thermo Fisher Scientific) instructions. Cell nuclei were counter-stained with DAPI (Calbiochem™, Merck) 1 mM at room temperature for 15 minutes. Stained section were visualized using fluorescent microscope (DMRXA, Leica Microsystems, Nanterre, France). The percentage of apoptotic cells was determined as the TUNEL-positive cell number divided by the respective total (DAPI-positive and TUNEL-positive) cell number, counting a minimum of 100 cells randomly analyzed per specimen.

Gene expression

NP samples were immediately snap-frozen in liquid nitrogen and stored at -80°C until further RNA extraction using ethanol precipitation. Each frozen specimen was pulverized using a ball mill (Tissue Lyser, Retsch, Eragny sur Oise, France). Total RNA was extracted using TRIzol according to the manufacturer's (Invitrogen™, Thermo Fisher Scientific) instructions. The quantity and purity of isolated total RNA were measured using spectrophotometry (SpectraMax™, Molecular Devices, San Jose, CA, USA). 4,000 ng of total RNA was reverse transcribed using the SuperScript™ II Reverse Transcriptase (Invitrogen™, Thermo Fisher Scientific) kit. Gene expression was then determined using 100 ng cDNA and TaqMan™ probes (Thermo Fisher Scientific) for anabolic genes (aggrecan (ACAN), collagen-I (COL1A1), collagen-II (COL2A1)), catabolic genes (a disintegrin and metalloprotease with thrombospondin type I repeats 4 and 5 (ADAMTS4, ADAMTS5), matrix metalloproteinases 3 and 13 (MMP3, MMP13)), protease inhibitor genes (tissue inhibitor of metalloproteinases 1 and 2 (TIMP1 and TIMP2)), NP cell phenotype genes (Brachyury (T), cytokeratin 8 (KRT8) and cytokeratin 18 (KRT18)), glucose transporter genes (GLUT-1 (SLC2A1), GLUT-3 (SLC2A3), and GLUT-4 (SLC2A4)), inflammatory mediator genes (interleukin 1β, 6, and 8 (IL1B, IL6 and CXCL8) and tumor necrosis factor α (TNF-α)), and senescence genes (p21 (CDKN1a) and p53 (TP53)). TaqMan™ assay IDs and the related reference gene sequences are listed in Table 1. Glyceraldehyde-3-phosphate dehydrogenase (GAPDH) gene was selected as reference gene from 5 tested genes (GAPDH, 18S, ribosomal protein L13a, hypoxanthine phosphoribosyltransferase 1, and peptidylprolyl isomerase A) as the most stable throughout the experimental conditions used in the present study. The results of gene expression levels are reported relative to the GAPDH expression level ($2^{-\Delta Ct}$ method).

Supernatant conditioned media analysis

At each cell culture medium change, aliquots of the supernatant conditioned media were collected, centrifuged, flash-frozen in liquid nitrogen, and preserved at -80°C until further analysis. The glucose and lactate content in each conditioned cell culture media were quantified using an automated analyzer (Respons910). The bovine IL-1β, IL-6, and TNF-α content in the conditioned culture media was quantified using the DuoSet ELISA kit according to the manufacturer's (R&D Systems, Minneapolis, MN, USA) instructions. The enzymatic activity of the MMPs released in the conditioned culture media was measured using the MMP Activity Assay Kit (Fluorometric–Green) according to the manufacturer's (Abcam, Cambridge, United Kingdom) instructions. MMP3 solution at 2,5 µg/mL in cell culture medium without FBS was used as a positive control.

Statistical analyses

All statistical analyses were performed using the GraphPad Prism Software v9.3.1 (GraphPad, Boston, MA, USA). Two-way ANOVA, followed by Tukey's post-hoc test, was used to examine the effects of glucose concentration, duration of cell culture, and their interaction; except for the TUNEL assay, where a t-test was conducted to investigate the effects of glucose concentration. For all statistical analyses, a p-value less than 0.05 was considered significant.

Results:

Effects of glucose depletion on NP cell viability and ECM content during 21 days of NP explant culture

Under healthy glucose conditions, the NP cell viability remained stable during the 21 days of culture (70% ± 6% at day 21, Fig.1a-b). In contrast, under degenerated glucose conditions, the NP cell viability decreased significantly ($p < 0.05$) on days 8, 12, and 21 (specifically, 46% ± 10%, 31% ± 9%, and 36% ± 12%, respectively). No necrotic centers were observed within the NP explants at any time point for the two glucose conditions tested in the present study.

The GAG content remained stable throughout the 21 days of NP explant culture and was similar for the two glucose conditions tested (Fig. 2a). The water and hydroxyproline contents decreased slightly and transiently on days 12 and 5, respectively, under the degenerated glucose condition (Fig. 2b-c).

Based on these results, NP cell fate and select functions were further investigated on days 1, 5, and 12, when NP cell viability was either not, slightly, or strongly affected by glucose depletion, respectively.

Effects of glucose depletion on NP cell fate during 12 days of NP explant culture

TUNEL staining confirmed the important decrease in NP cell viability after 12 days of culture under the degenerated compared to the healthy glucose condition (48% ± 11% vs. 20% ± 11% of TUNEL positive cells, respectively; Fig. 3a-b).

Gene expression levels of p21 (a.k.a. CDKN1A) and p53 senescence markers were stable and similar under the two glucose concentrations tested in the present study (Fig. 3c-d).

Gene expression levels of cytokeratin 8 and brachyury, two markers of healthy NP cell phenotype, tended to decrease under degenerated glucose conditions (Fig. 4a-c). These down regulations, however, were transient and did not reach statistical significance ($p > 0.05$).

Effect of glucose depletion on ECM anabolism and catabolism during 12 days of NP explant culture

With respect to ECM anabolism, aggrecan and collagen-II gene expression were both significantly ($p < 0.05$) reduced during culture under degenerated glucose conditions for 5 and 12 days when compared to expression levels at the beginning of the experiment (day 0) (Fig. 5a-b). In contrast, under healthy glucose conditions, the aggrecan gene expression levels remained stable, and the collagen-II gene expression was less and not significantly down-regulated (Fig. 5a-b). The collagen-I gene expression was not detected. The Safranin-O/Fast Green staining (Fig. 5c), however, showed a similar proteoglycan content between healthy and degenerated glucose conditions, confirming the previous biochemical assays (Fig. 2a).

Regarding the ECM catabolism, MMP activity in the supernatant conditioned culture media remained stable under the two glucose conditions investigated (Fig. 6a). The MMP3, MMP13, ADAMTS4, and ADAMTS5 gene expressions were not detected. Gene expression of TIMP1 and TIMP2 (MMP inhibitors) was similar under the two glucose conditions tested in the present study (Fig. 6b-c).

Effects of glucose depletion on glucose metabolism during 12 days of NP explant culture

For both healthy and degenerated glucose conditions, glucose was still present in the supernatant conditioned cell culture media at every medium change. Under the degenerated glucose condition, the glucose consumption ranged from 0.14 ± 0.02 mM on day 2 to 0.26 ± 0.02 mM on day 12 (Fig. 7a). Under the healthy glucose condition, glucose consumption changed from 0.94 ± 0.10 mM on day 2 to 1.17 ± 0.11 mM on day 12 (Fig. 7a), and was significantly ($p < 0.05$) higher than glucose consumption under degenerated glucose conditions at all time point of analysis. Accordingly, lactate production was significantly ($p < 0.05$) higher under healthy glucose conditions compared to the results obtained under degenerated glucose conditions (Fig. 7b). Gene expression of the glucose transporter GLUT-1 was stable and similar for both glucose conditions investigated (Fig. 7c). GLUT-3 gene expression was significantly higher at day 0 for the degenerated glucose condition, but after that remained stable and similar for both glucose conditions tested (Fig. 7d). GLUT-4 gene expression was not detected.

Effects of glucose depletion on inflammatory mediators during 12 days of NP explant culture

IL-1β, IL-6, and TNF-α concentrations in the supernatant conditioned cell culture media from the two glucose conditions tested in the present study were below the detection limits of the respective assays. The absence of inflammatory signals was further confirmed by the lack of gene expression of IL-1β, IL-6, IL-8, and TNF-α, which remained below the detection levels of the RT-qPCR assay used.

Discussion:

Using a physiological NP explant model, the present study showed that glucose depletion, as found in the degenerated IVD (i.e., 0.3 mM), has major deleterious effects on NP cell viability, minor negative effects on IVD matrix anabolism, and no impact on cellular senescence, ECM degradation, and inflammatory mediator production.

As previously reported in the literature in studies using isolated NP cells[16,19,24], glucose depletion had no effects on cell viability after 24 h (Fig. 1). NP cell viability, however, rapidly and extensively decreased when NP explants were cultured for longer periods with 0.3 mM of glucose, reaching 36% at day 21. These results are in accordance with studies using whole IVD organs exposed to limited nutritive conditions for 7 to 21 days and reporting extensive NP cell death in these conditions.[39,40] In these studies, however, limited nutritive conditions corresponded to cell culture medium containing 11 mM of glucose, and the actual level of glucose depletion to which NP cells are exposed in the core of IVD organs is unknown. Whole IVDs, moreover, were cultured in standard pH and oxygen conditions (7.4 and 21%, respectively), which could affect NP cell response to limited nutritive conditions.[26–28]

The drastic effect of glucose depletion on cell viability observed in the present study may be explained by the heavy reliance of NP cells on glycolysis. NP cell metabolism is, indeed,

highly glycolytic due to the avascular nature of the NP.[6,26] Glycolysis is a less efficient pathway than oxidative phosphorylation to produce energy, with 2 molecules of adenosine triphosphate (ATP) produced per molecule of glucose consumed for glycolysis vs. 36 molecules of ATP produced per molecule of glucose consumed for oxidative phosphorylation. Cells mainly relying on glycolysis, therefore, consume glucose at high rates in order to provide energy for cell metabolism. 0.3 mM of glucose may thus be insufficient to fuel glycolysis in NP cells to ensure cell survival, although NP explants of the present study never completely consumed glucose present in the cell culture media.

Interestingly, the present study provided evidence that glucose consumption by NP explants depended on the initial glucose concentration; on average, the NP cells consumed 63 ± 13% and 53 ± 7% of the initial 0.3 mM and 2 mM glucose concentrations, respectively (Fig.7a). Consumption of a relatively constant fraction of glucose in cell culture medium was also reported in studies on equine chondrocytes, a cell type phenotypically close to NP cells.[41] NP cells consumed 4.5-7 times more glucose in the healthy than in the degenerated glucose condition, which cannot be solely explained by a difference in viable NP cell density as this difference in glucose consumption was already observed at day 2 of culture (0.47 ± 0.05 mM/24 hours vs. 0.07 ± 0.01 mM/24 hours, respectively), when NP cells were viable in both glucose conditions. This observation may thus first suggest that glycolysis is restricted in the degenerated glucose condition. As facilitated glucose transport via GLUT (glucose transport) proteins is often the first rate-limiting step for glucose metabolism, the gene expression levels of class 1 GLUT-1, GLUT-3, and GLUT-4 were evaluated in the present study. GLUT-1 and GLUT-3 gene expressions were not affected by the glucose concentration in the cell culture medium; GLUT-4 expression was not detected (Fig. 7c-d). Other explanations for the higher glucose consumption by NP cells cultured in healthy glucose conditions might be either glucose storage in these cells (i.e., glycogenesis) or glucose use for proteoglycan production. The higher gene expression levels of aggrecan observed in the healthy glucose condition supports the latter explanation (Fig. 5a). Although glucose was never completely consumed in the present study, another explanation for the difference of glucose consumption between the glucose conditions may also be that NP cells adapted to a potential glucose shortage and used another energy source, such as L-glutamine, glycine or L-serine initially present in the cell culture media. A hypothesis supported by the mean mole ratio of lactate production:glucose consumption of 5:1 observed under degenerated glucose conditions, when the expected rate of glycolysis is 2:1. This observation indicates that the NP cells may produce energy from other carbon sources (such as amino acids present in the supernatant cell culture medium or degradation of intracellular components by autophagy)[42] under the degenerated glucose condition.

Contrary to cell viability, NP cell healthy phenotype was only slightly affected by glucose depletion in the present study. As observed in short-term studies using isolated NP cells[13,19,22,23], glucose depletion significantly ($p < 0.05$) reduced collagen-II and aggrecan gene expression at 5 and 12 days of NP explant culture (Fig. 5a-b). The fact that this gene expression down-regulation was not reflected at the protein level (i.e., stable GAG and HYP contents throughout the NP explant culture, Fig. 2a-c) can be explained by the activity of degradative enzymes too low (Fig. 6a) to degrade the initial high amounts of proteoglycan and collagen of NP explants in proportions detectable with the biochemical assays used in the present study. The fact that glucose depletion only tended to downregulate the gene expression of brachyury and cytokeratin 8 (Fig.4a and 4c), two putative phenotypical markers for healthy NP cells[43], however, suggests rather that glucose depletion has only a limited effect on NP cell healthy phenotype.

Glucose depletion also did not affect the MMP activity (Fig. 6a) nor the release of IL-1β, IL-6, and TNF-α (data not shown) in supernatant cell culture media in the present study. As RT-qPCR analysis confirmed the absence of MMP3, MMP13, ADAMTS4, ADAMTS5, IL-1β, IL-6, and TNF-α gene expression, these results provided evidence that glucose depletion alone is insufficient to trigger the degenerative or the inflammatory cascade in NP cells. These results contradict the increased gene expression of IL-6 and IL-8 observed in whole IVD organs cultured under limited nutritive conditions.[44] This disparity may be explained by the addition of mechanical loading or by the unknown level of glucose depletion used in this whole IVD organ culture system, as discussed before. The absence of ECM degradation or inflammation induction by glucose depletion in the present study may be related to the lack of increased gene expression of senescence molecular markers (i.e., p53 and p21; Fig. 3b-c). Senescent disc cells, indeed, enhance both the disc ECM degradation and the secretion of pro-inflammatory cytokine secretion through senescence-associated secretory phenotype.[45]

The main limitation of the present study is that the NP explant culture system used did not include mechanical stimulation: NPs are physiologically exposed to a range of mechanical loading, specifically, from 100 kPa in the prone position to 1,700 kPa in weight-bearing humans.[46]Adding mechanical stimulation to the NP explant culture system used in the present study may thus affect the observed results. Physiological dynamic compression (0.1 to 2 Hz of 4 to 15% of strain magnitude for 4 hours) of NP cells seeded into hydrogels, however, either did not or slightly affected glucose consumption and lactate production and collagen-II and aggrecan gene expression compared to unloaded controls.[22,47–50]

Conclusion:

To conclude, the present study distinctively demonstrated that glucose depletion in a physiologically pertinent model leads to diminished cell viability without triggering the degenerative phenotype of NP cells. This observation suggests that glucose depletion is not the only micro-environmental factor involved in IVD degeneration onset. Moreover, although NP cells seem to adapt to glucose shortage by using other carbon sources, the present study's results call for caution regarding nutrient supply when developing therapeutical strategies for IVD repair.

Acknowledgments:

The authors would like to thank Prof R. Bizios for reviewing the manuscript and Dr. E. Masson for the osmolarity measurements. This work was funded by Agence Nationale de la Recherche (ANR-18-CE18-0004) and by Fondation de l'Avenir (AP-RM-17-006). The authors confirm that there are no known conflicts of interest associated with this publication and there has been no significant financial support for this work that could have influenced its outcome.

Disclosure Statement:

The authors declare no competing financial interests

References:

1. Global Burden of Disease Study 2017 Collaborators. 2018. Global, regional, and national incidence, prevalence, and years lived with disability for 354 diseases and injuries for 195 countries and territories, 1990-2017: a systematic analysis for the Global Burden of Disease Study 2017. Lancet 392(10159):1789–1858.

2. Hoy D, March L, Brooks P, et al. 2014. The global burden of low back pain: estimates from the Global Burden of Disease 2010 study. Ann. Rheum. Dis. 73(6):968–974.

3. Luoma K, Riihimäki H, Luukkonen R, et al. 2000. Low back pain in relation to lumbar disc degeneration. Spine 25(4):487–492.

4. Aavikko A, Lohman M, Ristolainen L, et al. 2022. ISSLS prize in clinical science 2022: accelerated disc degeneration after pubertal growth spurt differentiates adults with low back pain from their asymptomatic peers. Eur. Spine J. 31(5):1080–1087.

5. Kepler CK, Ponnappan RK, Tannoury CA, et al. 2013. The molecular basis of intervertebral disc degeneration. Spine J. 13(3):318–330.

6. Holm S, Maroudas A, Urban JPG, et al. 1981. Nutrition of the intervertebral disc: solute transport and metabolism. Connect. Tissue Res. 8(2):101–119.

7. Jackson AR, Huang C-YC, Brown MD, Yong Gu W. 2011. 3D finite element analysis of nutrient distributions and cell viability in the intervertebral disc: effects of deformation and degeneration. J. Biomech. Eng. 133(9):091006.

8. Sélard É, Shirazi-Adl A, Urban JPG. 2003. Finite element study of nutrient diffusion in the human intervertebral disc. Spine 28(17):1945–1953.

9. Soukane D, Shirazi-Adl A, Urban JPG. 2007. Computation of coupled diffusion of oxygen, glucose and lactic acid in an intervertebral disc. J. Biomech. 40(12):2645–2654.

10. Kitano T, Zerwekh JE, Usui Y, et al. 1993. Biochemical changes associated with the symptomatic human intervertebral disk. Clin. Orthop. (293):372–377.

11. Fields AJ, Ballatori A, Liebenberg EC, Lotz JC. 2018. Contribution of the endplates to disc degeneration. Curr. Mol. Biol. Rep. 4(4):151–160.

12. Bartels EM, Fairbank JC, Winlove CP, Urban JP. 1998. Oxygen and lactate concentrations measured in vivo in the intervertebral discs of patients with scoliosis and back pain. Spine 23(1):1–7; discussion 8.

13. Yin X, Motorwala A, Vesvoranan O, et al. 2020. Effects of glucose deprivation on ATP and proteoglycan production of intervertebral disc cells under hypoxia. Sci. Rep. 10(1):8899.

14. Shirazi-Adl A, Taheri M, Urban JPG. 2010. Analysis of cell viability in intervertebral disc: Effect of endplate permeability on cell population. J. Biomech. 43(7):1330–1336.

15. Wu Y, Cisewski S, Sachs BL, Yao H. 2013. Effect of cartilage endplate on cell based disc regeneration: a finite element analysis. Mol. Cell. Biomech. MCB 10(2):159–182.

16. Bibby SRS, Urban JPG. 2004. Effect of nutrient deprivation on the viability of intervertebral disc cells. Eur. Spine J. 13(8):695–701.

17. Guehring T, Wilde G, Sumner M, et al. 2009. Notochordal intervertebral disc cells: Sensitivity to nutrient deprivation. Arthritis Rheum. 60(4):1026–1034.

18. Johnson WEB, Stephan S, Roberts S. 2008. The influence of serum, glucose and oxygen on intervertebral disc cell growth in vitro: implications for degenerative disc disease. Arthritis Res. Ther. 10(2):R46.

19. Neidlinger-Wilke C, Mietsch A, Rinkler C, et al. 2012. Interactions of environmental conditions and mechanical loads have influence on matrix turnover by nucleus pulposus cells. J. Orthop. Res. 30(1):112–121.

20. Chang H, Wang H, Yang X, et al. 2021. Comprehensive profile analysis of differentially expressed circRNAs in glucose deprivation-induced human nucleus pulposus cell degeneration. BioMed Res. Int. 2021:1–14.

21. Liu J, Yuan C, Pu L, Wang J. 2017. Nutrient deprivation induces apoptosis of nucleus pulposus cells via activation of the BNIP3/AIF signalling pathway. Mol. Med. Rep. 16(5):7253–7260.

22. Rinkler C, Heuer F, Pedro MT, et al. 2010. Influence of low glucose supply on the regulation of gene expression by nucleus pulposus cells and their responsiveness to mechanical loading: Laboratory investigation. J. Neurosurg. Spine 13(4):535–542.

23. Wang Y, Yang Y, Zuo R, et al. 2020. FOXO3 protects nucleus pulposus cells against apoptosis under nutrient deficiency via autophagy. Biochem. Biophys. Res. Commun. 524(3):756–763.

24. Saggese T, Thambyah A, Wade K, McGlashan SR. 2020. Differential response of bovine mature nucleus pulposus and notochordal cells to hydrostatic pressure and glucose restriction. Cartilage 11(2):221–233.

25. Naqvi SM, Buckley CT. 2015. Extracellular matrix production by nucleus pulposus and bone marrow stem cells in response to altered oxygen and glucose microenvironments. J. Anat. 227(6):757–766.

26. Bibby SRS, Jones DA, Ripley RM, Urban JPG. 2005. Metabolism of the intervertebral disc: effects of low levels of oxygen, glucose, and pH on rates of energy metabolism of bovine nucleus pulposus cells. Spine 30(5):487–496.

27. Huang C-YC, Yuan T-Y, Jackson AR, et al. 2007. Effects of low glucose concentrations on oxygen consumption rates of intervertebral disc cells. Spine 32(19):2063–2069.

28. Horner HA, Urban JP. 2001. 2001 Volvo award winner in basic science studies: Effect of nutrient supply on the viability of cells from the nucleus pulposus of the intervertebral disc. Spine 26(23):2543–2549.

29. Rosenzweig DH, Tremblay Gravel J, Bisson D, et al. 2017. Comparative analysis in continuous expansion of bovine and human primary nucleus pulposus cells for tissue repair applications. Eur. Cell. Mater. 33:240–251.

30. Hynes RO. 2009. The extracellular matrix: not just pretty fibrils. Science 326(5957):1216–1219.

31. Bonnans C, Chou J, Werb Z. 2014. Remodelling the extracellular matrix in development and disease. Nat. Rev. Mol. Cell Biol. 15(12):786–801.

32. Hynes RO. 2002. Integrins: bidirectional, allosteric signaling machines. Cell 110(6):673–687.

33. Chang C. 2016. Agonists and antagonists of TGF-β family ligands. Cold Spring Harb. Perspect. Biol. 8(8):a021923.

34. van Dijk B, Potier E, Ito K. 2011. Culturing bovine nucleus pulposus explants by balancing medium osmolarity. Tissue Eng. Part C Methods 17(11):1089–1096.

35. van Dijk BGM, Potier E, Ito K. 2013. Long-term culture of bovine nucleus pulposus explants in a native environment. Spine J. 13(4):454–463.

36. Schindelin J, Arganda-Carreras I, Frise E, et al. 2012. Fiji: an open-source platform for biological-image analysis. Nat. Methods 9(7):676–682.

37. Farndale R, Buttle D, Barrett A. 1986. Improved quantitation and discrimination of sulphated glycosaminoglycans by use of dimethylmethylene blue. Biochim. Biophys. Acta 883(2):173–177.

38. Huszar G, Maiocco J, Naftolin F. 1980. Monitoring of collagen and collagen fragments in chromatography of protein mixtures. Anal. Biochem. 105(2):424–429.

39. Illien-Jünger S, Gantenbein-Ritter B, Grad S, et al. 2010. The combined effects of limited nutrition and high-frequency loading on intervertebral discs with endplates. Spine 35(19):1744–1752.

40. Jünger S, Gantenbein-Ritter B, Lezuo P, et al. 2009. Effect of limited nutrition on in situ intervertebral disc cells under simulated-physiological loading. Spine 34(12):1264–1271.

41. Schneider N, Mouithys-Mickalad A, Lejeune J-P, et al. 2007. Oxygen consumption of equine articular chondrocytes: Influence of applied oxygen tension and glucose concentration during culture. Cell Biol. Int. 31(9):878–886.

42. Kritschil R, Scott M, Sowa G, Vo N. 2022. Role of autophagy in intervertebral disc degeneration. J. Cell. Physiol. 237(2):1266–1284.

43. Risbud MV, Schoepflin ZR, Mwale F, et al. 2015. Defining the phenotype of young healthy nucleus pulposus cells: Recommendations of the Spine Research Interest Group at the 2014 annual ORS meeting. J. Orthop. Res. 33(3):283–293.

44. Lang G, Liu Y, Geries J, et al. 2018. An intervertebral disc whole organ culture system to investigate proinflammatory and degenerative disc disease condition. J. Tissue Eng. Regen. Med. 12(4):e2051–e2061.

45. Feng C, Liu H, Yang M, et al. 2016. Disc cell senescence in intervertebral disc degeneration: Causes and molecular pathways. Cell Cycle 15(13):1674–1684.

46. Wilke H-J, Neef P, Hinz B, et al. 2001. Intradiscal pressure together with anthropometric data – a data set for the validation of models. Clin. Biomech. 16:S111–S126.

47. Fernando HN, Czamanski J, Yuan T-Y, et al. 2011. Mechanical loading affects the energy metabolism of intervertebral disc cells. J. Orthop. Res. 29(11):1634–1641.

48. Salvatierra JC, Yuan TY, Fernando H, et al. 2011. Difference in energy metabolism of annulus fibrosus and nucleus pulposus cells of the intervertebral disc. Cell. Mol. Bioeng. 4(2):302–310.

49. Korecki CL, Kuo CK, Tuan RS, Iatridis JC. 2009. Intervertebral disc cell response to dynamic compression is age and frequency dependent. J. Orthop. Res. 27(6):800–806.

50. Wuertz K, Urban JPG, Klasen J, et al. 2007. Influence of extracellular osmolarity and mechanical stimulation on gene expression of intervertebral disc cells. J. Orthop. Res. 25(11):1513–1522.

Corresponding author:
Dr Esther POTIER PhD
Laboratory B3OA UMR CNRS 7052 INSERM U1271, Fac Médecine - Univ Paris Cité -Site Villemin, 10 Avenue de Verdun, 75010 Paris, France
Phone number: 0033.1.57.27.85.70
Fax: 0033.1.57.27.85.71
E-mail:esther.potier@cnrs.fr

To cite this article:
Mathilde PADRONA, Manon MAROQUENNE, Hanane EL-HAFCI, Lucille ROSSIAUD1, Hervé PETITE, and Esther POTIER, Glucose Depletion Decreases Cell Viability Without Triggering Degenerative Changes In A Physiological Nucleus Pulposus, Journal of Orthopaedic Research, Ref DOI: 10.1002/jor.25742

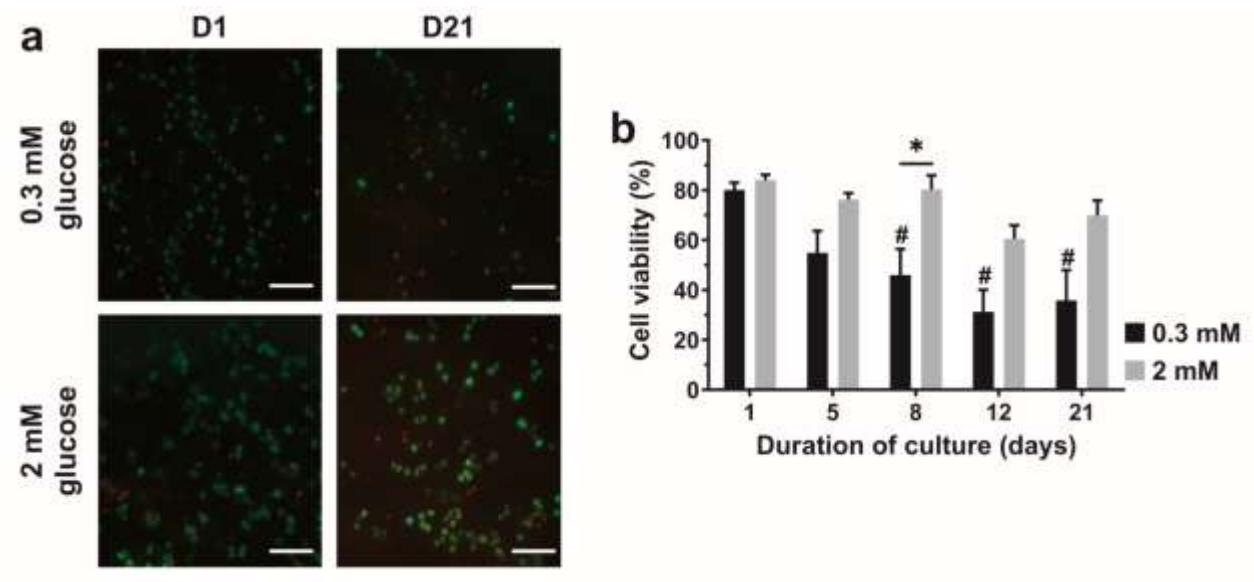

Figure 1: Cell viability of bovine NP explants cultured for 21 days in either healthy (2 mM) or degenerated (0.3 mM) glucose conditions. (**a**) Representative confocal images of NP cell viability at day 1 (D1) and day 21 (D21) of NP explant culture using calcein staining for living cells (green) and propidium iodide staining for dead cells (red). Scale bar = 100 μm. (**b**) Quantification of NP cell viability. Values are mean + Standard Error of the Mean (SEM); n = 5-8 donors. * $p < 0.05$; # $p < 0.05$ vs. respective D1.

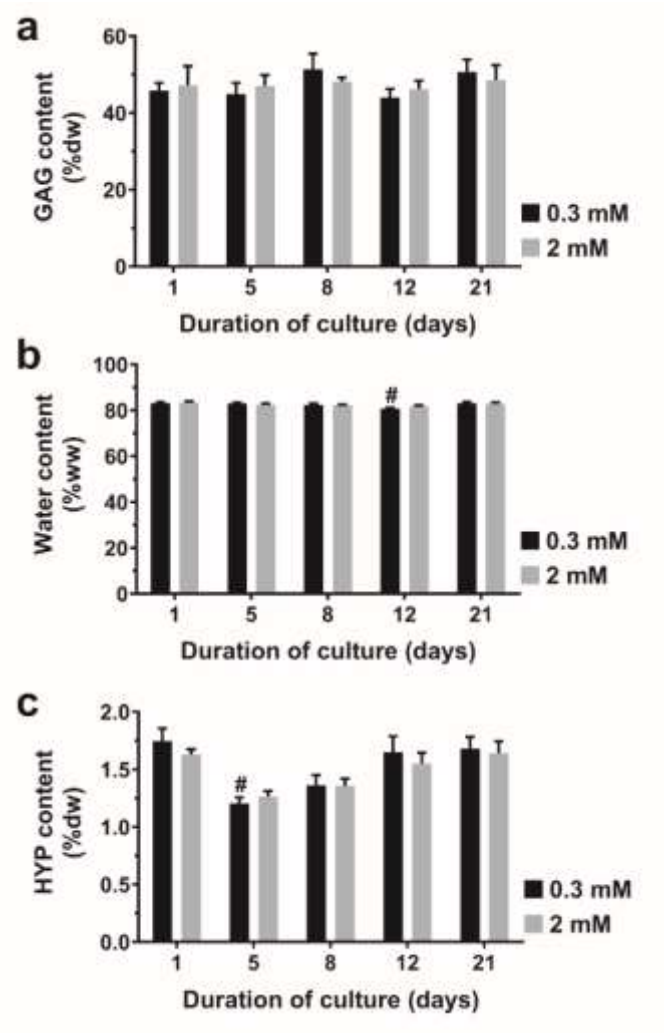

Figure 2: Extracellular matrix characterization of bovine NP explants cultured for 21 days in either healthy (2 mM) or degenerated (0.3 mM) glucose conditions. (**a**) Glycosaminoglycan (GAG) content, expressed as a percentage dry weight (% dw). (**b**) Water content expressed as a percentage of wet weight (% ww). (**c**) Hydroxyproline (HYP) content expressed as percentage of dry weight (% dw). Values are mean + Standard Error of the Mean (SEM); n = 5-8 donors. # $p < 0.05$ vs. respective D1.

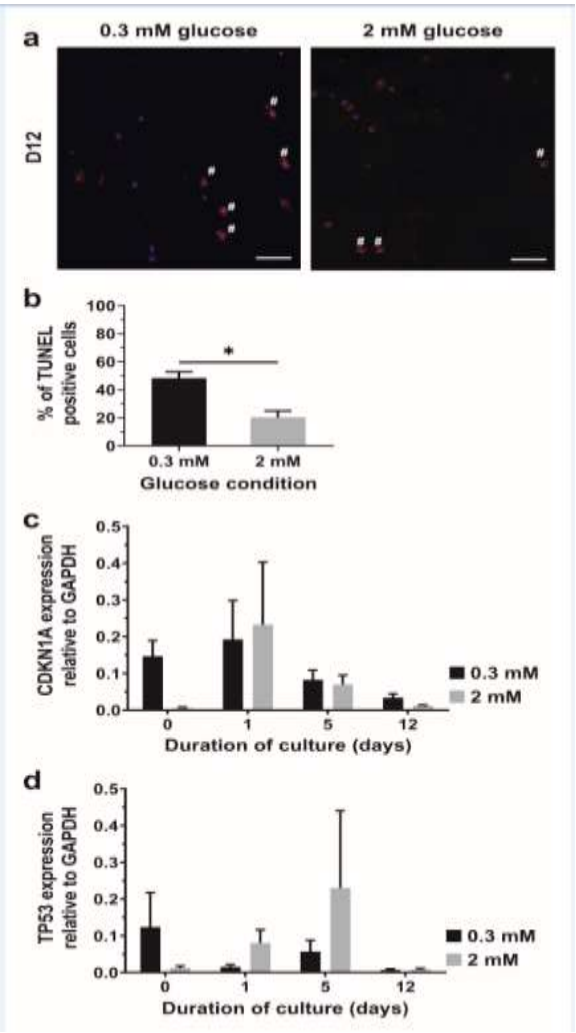

Figure 3: Apoptosis and senescent markers of bovine NP explants cultured for 12 days in either healthy (2 mM) or degenerated (0.3 mM) glucose conditions. (**a**) Representative images of immunostaining results using TUNEL for apoptotic cells (red fluorescence) and DAPI staining for cell nuclei (blue fluorescence). The # symbol indicates positive TUNEL cells. Scale bar = 50 µm. (**b**) Quantification of TUNEL positive cells. Expression levels of the senescence genes (**c**) p21 (CDKN1A) and (**d**) p53 (TP53) relative to GAPDH ($2^{-\Delta Ct}$ method). Values are mean + Standard Error of the Mean (SEM); n = 4-6 donors. * $p < 0.05$.

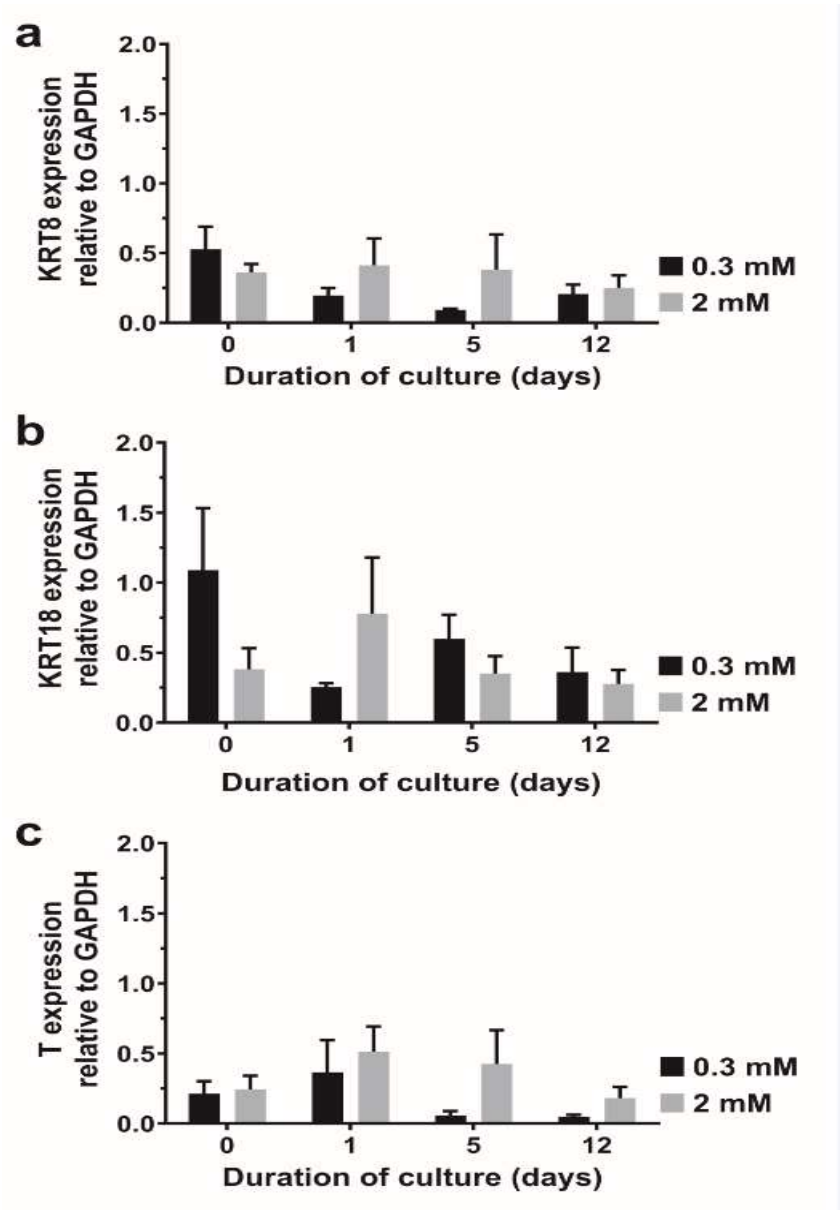

Figure 4: NP cell phenotype markers of bovine NP explants cultured for 12 days in either healthy (2 mM) or degenerated (0.3 mM) glucose conditions. Expression levels of the (**a**) cytokeratin 8 (KRT8), (**b**) cytokeratin 18 (KRT18), and (**c**) brachyury (T) genes relative to GAPDH ($2^{-\Delta Ct}$ method). Values are mean + Standard Error of the Mean (SEM); n = 4-6 donors.

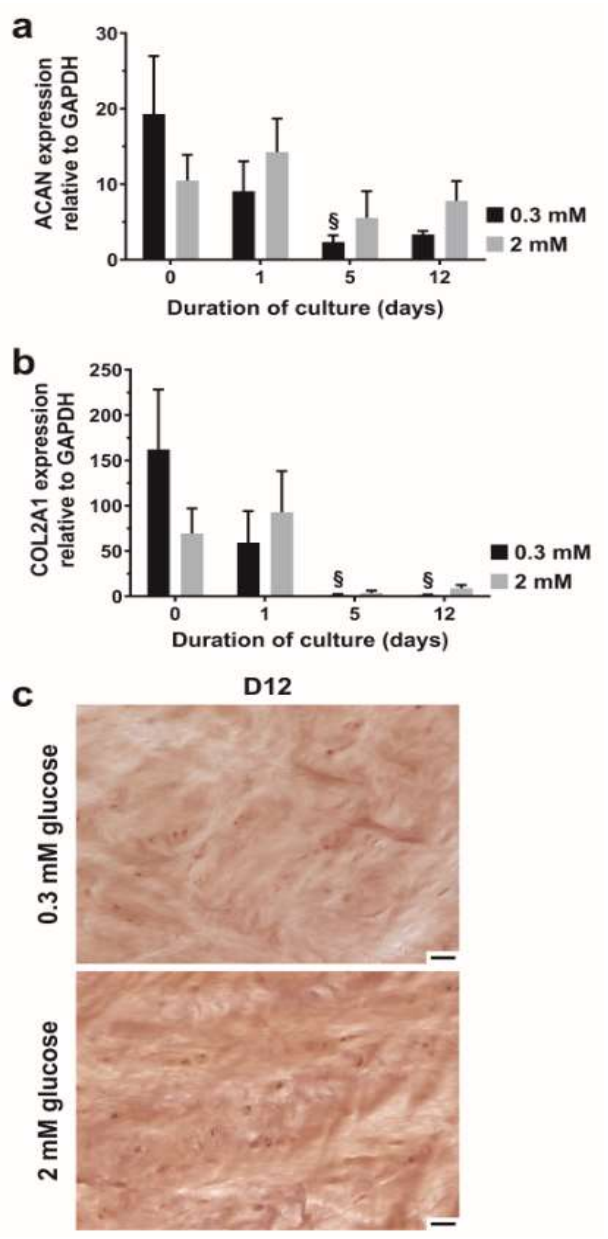

Figure 5: ECM anabolism of bovine NP explants cultured for 12 days in either healthy (2 mM) or degenerated (0.3 mM) glucose conditions. Expression levels of the anabolic genes (**a**) aggrecan (ACAN) and (**b**) collagen-II (COL2A1) relative to GAPDH ($2^{-\Delta Ct}$ method). Values are mean + Standard Error of the Mean (SEM); n = 4-5 donors. § $p < 0.05$ vs. respective D0. (**c**) Representative light microscopy images of ECM stained with Safranin-O for proteoglycan (red/orange), Fast Green for collagen (green), and Weigert's Iron Hematoxylin for cell nuclei (black) visualization after 12 days (D12) of culture. Scale bar = 50 µm.

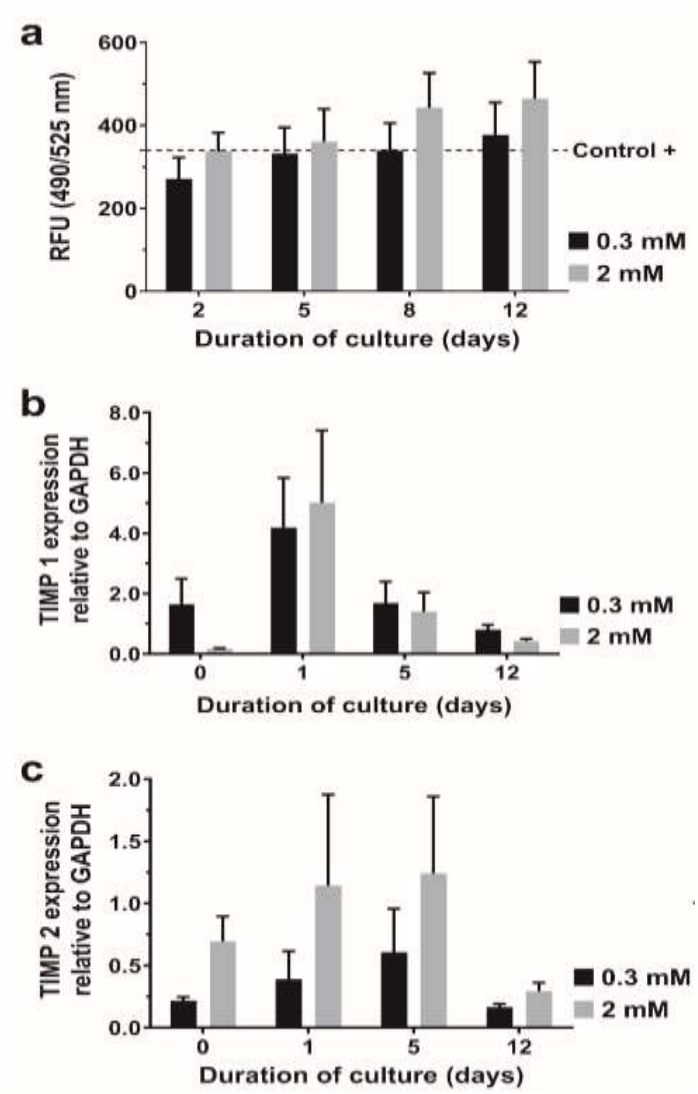

Figure 6: ECM catabolism of bovine NP explants cultured for 12 days in either healthy (2 mM) or degenerated (0.3 mM) glucose conditions. (**a**) Total matrix metalloproteinase (MMP) activity (relative fluorescent unit, RFU) in the supernatant conditioned cell culture media. Expression levels of the catabolic genes (**b**) tissue inhibitor of metalloproteinases 1 (TIMP1) and (**c**) tissue inhibitor of metalloproteinases 2 (TIMP2) relative to GAPDH ($2^{-\Delta Ct}$ method). Values are mean + Standard Error of the Mean (SEM); n = 4-6 donors.

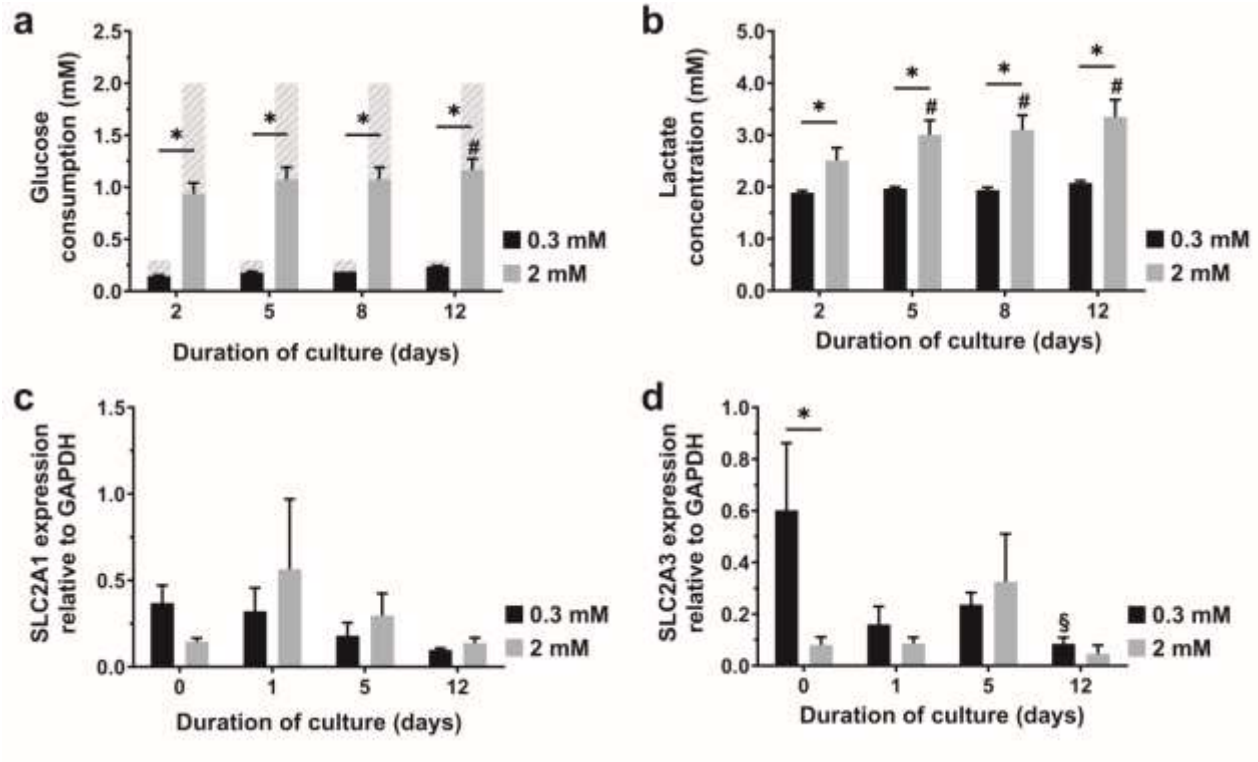

Figure 7: Glucose metabolism of bovine NP explants cultured for 12 days in either healthy (2 mM) or degenerated (0.3 mM) glucose conditions. (**a**) Glucose consumption and (**b**) Lactate production in supernatant conditioned cell culture media. The striped zones on frame (a) indicate the initial glucose concentration in the cell culture media. Expression levels of the glucose transporters (**c**) GLUT-1 (SLC2A1) and (**d**) GLUT-3 (SLC2A3) genes relative to GAPDH ($2^{-\Delta Ct}$method). Values are mean + Standard Error of the Mean (SEM); n = 4-6 donors; * $p < 0.05$; # $p < 0.05$ vs. respective D2; § $p < 0.05$ vs. respective D0.

Gene name (symbol)	TaqMan™ assay ID	Product size (bp)	NCBI reference sequence
Aggrecan (ACAN)	Bt03212186_m1	55	NM_173981.2
Collagen type I alpha 1 chain (COL1A1)	Bt03225322_m1	65	NM_001034039.2
Collagen type II alpha 1 chain (COL2A1)	Bt03251861_m1	54	NM_001001135.3
ADAM metallopeptidase with thrombospondin type 1 motif 4 (ADAMTS4)	Bt03224697_m1	59	NM_181667.1
ADAM metallopeptidase with thrombospondin type 1 motif 5 (ADAMTS5)	Bt04230785_m1	75	NM_001166515.1
Matrix metallopeptidase 3 (MMP3)	Bt04259490_m1	76	NM_001206637.1
Matrix metallopeptidase 13 (MMP13)	Bt03214050_m1	68	NM_174389.2
TIMP metallopeptidase inhibitor 1 (TIMP1)	Bt03223720_m1	55	NM_174471.3
TIMP metallopeptidase inhibitor 2 (TIMP2)	Bt03231007_m1	88	NM_174472.4
T-box transcription factor T (T)	Bt04313977_m1	83	NM_001192985.1
Keratin 8 (KRT8)	Bt03225175_g1	78	NM_001033610.1
Keratin 18 (KRT18)	Bt00989202_g1	58	NM_001192095.1
Solute carrier family 2 member 1 (SLC2A1)	Bt03215313_m1	55	NM_174602.2
Solute carrier family 2 member 3 (SLC2A3)	Bt03259519_gH	62	NM_174603.3
Solute carrier family 2 member 4 (SLC2A4)	Bt03215316_m1	69	NM_174604.1
Interleukin 1 beta (IL1B)	Bt03212741_m1	71	NM_174093.1
Interleukin 6 (IL6)	Bt03211905_m1	115	NM_173923.2
C-X-C motif chemokine ligand 8 (CXCL8)	Bt03211906_m1	114	NM_173925.2
Tumor necrosis factor (TNF-α)	Bt03259156_m1	69	NM_173966.3
Cyclin dependent kinase inhibitor 1A (CDKN1a)	Bt03262189_m1	63	NM_001098958.2
Tumor protein p53 (TP53)	Bt03223222_m1	66	NM_174201.2
Glyceraldehyde-3-phosphate dehydrogenase (GAPDH)	Bt03210913_g1	66	NM_001034034.2

Table 1: List of TaqMan™ Gene Expression Assays